THE DYNAMICAL BEHAVIOR OF A MAGNETIC FLUID FLOW IN A CYLINDRICAL TUBE

Douglas Machado Ramos
Departamento de Engenharia Mecânica, Faculdade de Tecnologia, Universidade de Brasília, Campus Universitário Darcy Ribeiro, 70910-900 Brasília-DF, Brazil.
douglasmramos@yahoo.com.br

Francisco Ricardo da Cunha, (corresponding author)
frcunha@unb.br

José Luiz Alves da Fontoura Rodrigues
fontoura@unb.br

Abstract. *Simulations results of laminar flow of a magnetic fluid under action of steady and oscillating non-uniform magnetic fields are presented and discussed. A finite volume method is applied in order to discretize the governing coupled equations of hydrodynamics and magneto-static. The appropriated boundary conditions for velocity, magnetization and field intensity on the cylindrical tube wall are imposed and the relevant physical parameters of the flow identified. The influence of those parameters on the fluid proprieties and the flow instabilities and bifurcations is investigated. The behavior of the magnetic fluid is explored for different nano-particle volume fractions and several magnetization relaxation times. The non-linear response of the flow under several magnetic conditions is presented in terms of pressure times series, phase diagrams and spectrum of fluctuations. The amplitudes of the velocity fluctuations in an oscillatory field are also evaluated by our numerical simulations.*

Keywords: *Numerical simulation, Magnetic Fluid, Finite Volume Method, Laminar pipe flow.*

1. Introduction

Magnetic fluids are colloidal suspensions of fine particles of solid ferromagnetic material in a carrier liquid. The flow of such kind of fluid is affected by the presence of applied external magnetic fields. In the absence of magnetic fields the fluid flow down a circular tube shows the familiar parabolic Poiseuille pattern. If an uniform steady magnetic field is applied along the tube for the same pressure gradient the flow pattern remains parabolic but the flow rate is strongly reduced (Felderhof, 2001). In the absence of magnetic field gradient the magnetic force is null. The particles however, cannot rotate with the vorticity of fluid due to the resistance imposed by the magnetic polarization. This resistance is interpreted as an increasing in the fluid viscosity. In the case of a non-zero positive magnetic gradient the magnetic force is positive and the flow rate increases.

Despite the simplicity of the geometry of laminar flow in pipes the flow structure of magnetic fluids is complex due to the nonlinear coupling between hydrodynamics and magnetism. The laminar flow of magnetic fluids has been subject of several studies. Felderhof (2001) has examined the flow of ferrofluids down a tube in an oscillating magnetic field and analyzed a set of magnetization evolution equations, Cunha & Sobral (2004) proposed a simplified evolution equation for the fluid magnetization and solved the pressure driven pipe-flow problem by using asymptotical theory. The numerical modelling of magnetic fluid instabilities has been explored by Oldenburg et al. (2000), Berthier & Ricoul (2002) and Ramos et al. (2004, 2005). Many experimental observations on the behavior of magnetic fluids have been carried out by Kamiama et al. (1992) and Fannin (1994).

The purpose of this work is to investigate the flow of a magnetic fluid in a cylindrical tube under action of steady and oscillating non-uniform magnetic fields by numerical simulations based on the solution of the coupled magnetic-hydrodynamic governing equations. The influence of particle volume fraction and magnetization relaxation time are examined by using uniform or non-uniform steady applied magnetic fields. Oscillating non-uniform magnetic fields are prescribed in order to determine the flow response in terms of pressure and velocity fluctuations.

2. Governing equations

The magnetic fluid flow problem falls naturally into two parts: that of finding the internal magnetic field and the fluid magnetization, and that of determining the fluid motion variables (velocity and pressure). In this section we present the equations which the magnetic and the hydrodynamic fields everywhere satisfy.

The orientation of dipole moments of individual colloidal particles in a liquid is randomized by Brownian motion in the absence of a magnetic field. Super-paramagnetic particles behave without hysteresis in dilute magnetic fluids, when no interaction among neighbors are presented. Thus the fluid does not have memory and the local magnetization is allowed to be instantaneously oriented in the direction of the local magnetic field. Under these conditions the magnetization field is collinear with the local magnetic field, that implies: $\boldsymbol{M} \times \boldsymbol{H} = \boldsymbol{0}$. Since the movement of electrical charges is absent, the Ampère-Maxwell's law is reduced to:

$$\nabla \times \boldsymbol{H} = \boldsymbol{0}\,, \tag{1}$$

therefore the local magnetic field $\boldsymbol{H}$ may be determined by mean of a magnetic potential ϕ_m, namely:

$$\boldsymbol{H} = \nabla\phi_m \,. \tag{2}$$

The induced field is defined as

$$\boldsymbol{B} = \mu_0\left(\boldsymbol{H} + \boldsymbol{M}\right) \,, \tag{3}$$

where $\mu_0 = 4\pi \times 10^{-4}\mathrm{H}\cdot\mathrm{m}^{-1}$ is the vacuum magnetic permeability. The magnetism Gauss's law for the induced magnetic field $\boldsymbol{B}$ is simply

$$\nabla\cdot\boldsymbol{B} = 0 \,. \tag{4}$$

Substituting Eq. (3) in Eq. (4) and using Eq. (2), it obtains a Poisson's equations for ϕ_m

$$\nabla^2\phi_m = -\nabla\cdot\boldsymbol{M} \,. \tag{5}$$

The magnetization field $\boldsymbol{M}$ for a dilute magnetic fluid with $\boldsymbol{M}\times\boldsymbol{H} = \boldsymbol{0}$ is determined by the evolution equation proposed by Cunha & Sobral (2004)

$$\frac{\partial\boldsymbol{M}}{\partial t} + \boldsymbol{u}\cdot\nabla\boldsymbol{M} = \boldsymbol{\Omega}\times\boldsymbol{M} - \frac{\boldsymbol{1}}{\tau_{\mathbf{s}}}\left(\boldsymbol{M} - \boldsymbol{M^o}\right) \,, \tag{6}$$

where $\boldsymbol{u}$ is the Eulerian velocity, τ_s is the magnetic relaxation time of the particles and $\boldsymbol{\Omega} = \frac{\boldsymbol{1}}{\boldsymbol{2}}\nabla\times\boldsymbol{u}$ represents the angular fluid velocity. The quantity $\boldsymbol{M^o}$ denotes the equilibrium magnetization for a quiescent magnetic fluid. For very dilute suspensions, the equilibrium magnetization is collinear with the local field $\boldsymbol{H}$ and it is determined by a Langevin function (Rosensweig, 1997):

$$M^o = \phi M_d\mathcal{L}(\gamma) = \phi M_d\left(\coth\gamma - \gamma^{-1}\right) \,, \tag{7}$$

with the dimensionless parameter γ defined as:

$$\gamma = \frac{3\chi_o}{\phi M_d}H = \frac{mH}{k_B T} \,. \tag{8}$$

Here $\boldsymbol{M^o} = M^o\boldsymbol{H}/H$, $H = |\boldsymbol{H}|$ and $M^o = |\boldsymbol{M^o}|$. The propriety M_d in Eq. (7) represents the bulk magnetization of the particle and ϕ is the volume fraction of the magnetic particles. In Eq. (8) the quantity $\chi_o = M/H_o$ is the magnetic susceptibility based on the applied field H_o, m denotes the dipole moment of the particles, $k_B = 1.38\times10^{-23}$J/K is the Boltzmann constant and T is the absolute temperature. The parameter γ, usually called the energy ratio parameter represents the relation between the magnetic energy mH and the thermal energy k_BT associated to the motion of a magnetic particle. The first term on the right hand side of Eq. (6) represents the change in the magnetization of a particle due to the local rotation of the fluid, whereas the second one states for the deviation from the equilibrium magnetization in a quiescent fluid.

Cunha & Sobral (2004) have considered an evolution equation for the magnetization in which the relevant terms are just the ones associated with particle rotation and the deviation from the equilibrium. This condition corresponds to a quasi-steady regime for the magnetization, that means changes in this quantity occur instantaneously compared with a typical time scale of the flow. For this case, changes in the magnetization of the fluid are consequence of the flow vorticity only, and Eq. (6) reduces to

$$\Omega\times\boldsymbol{M} = \frac{1}{\tau_s}\left(\boldsymbol{M} - \boldsymbol{M^o}\right) \,. \tag{9}$$

Hydrodynamic balance equations are also needed for this coupled problem. The continuity equation for an incompressible fluid is given by:

$$\nabla\cdot\boldsymbol{u} = 0 \,, \tag{10}$$

When internal torques are absent in the flow, the stress tensor is symmetric and the balance of linear momentum for a continuum magnetic fluid is given by:

$$\rho\left(\frac{\partial\boldsymbol{u}}{\partial t} + \boldsymbol{u}\cdot\nabla\boldsymbol{u}\right) = -\nabla p + \eta^*\nabla^2\boldsymbol{u} + \mu_0\boldsymbol{M}\cdot\nabla\boldsymbol{H} \,, \tag{11}$$

where ρ is the density, p denotes the pressure modified by gravitational effects and η^* is the effective viscosity of the magnetic fluid depending on hydrodynamic and magnetic effects. The last term on the right hand side of Eq. (11) represents the magnetic forces acting in the fluid particles and is proportional to the magnetization and the local magnetic field gradient.

The fluid viscosity depends on the particle volume fraction and the particle dipole orientation due to the alignment with the magnetic field. If no-magnetic field is applied the effective viscosity is purely hydrodynamic and its $O(\phi)$ may be determined by the equation proposed by Einstein (1956) for an infinitely dilute suspension

$$\eta = \eta_0\left(1 + \frac{5}{2}\phi\right) + O(\phi^2) \,, \tag{12}$$

where η_0 is the viscosity of the suspending fluid. The $O(\phi^2)$ is a non-newtonian effect related to the hydrodynamic interactions between the particles. A general empirical formula is proposed by Kreiger-Taylor (see Barnes, Hutton & Walters, 1989),

$$\frac{\eta}{\eta_0} = \left(1 - \frac{\phi}{\phi_{max}}\right)^{-[\eta]\phi_{max}} \,, \tag{13}$$

where $[\eta]$ is the intrinsic viscosity associated with the particle diameter and ϕ_{max} denotes the maximum packing factor of spherical particles. For submicron particles $[\eta] \sim 5/2$ and $\phi_{max} \sim 7/10$ (Barnes et al., 1989). For dilute suspensions where $\phi/\phi_{max} \ll 1$, Eq. (13) can be represented by a binomial serie as following

$$\frac{\eta}{\eta_0} \sim 1 + [\eta]\phi + \frac{[\eta]\phi_{max}\left([\eta]\phi_{max}+1\right)}{2}\left(\frac{\phi}{\phi_{max}}\right)^2 + \\ - \frac{[\eta]\phi_{max}\left([\eta]\phi_{max}+1\right)\left([\eta]\phi_{max}+2\right)}{6}\left(\frac{\phi}{\phi_{max}}\right)^3 + \ldots \tag{14}$$

It should important to note that equation (14) is reduced to Eq. (12) for $\phi \to 0$.

In the presence of an applied field the particles cannot rotate freely with the fluid vorticity due to the particle magnetization. In this case an extra correction $O(\phi)$ in η must be considered

$$\eta^* = \eta + \Delta\eta \, , \tag{15}$$

where $\Delta\eta$ is the viscosity increment due to magnetic effects. The $O(\phi)$ correction for the viscosity of a magnetic fluid may be expressed as

$$\eta^* = \eta_0 \left\{1 + \left[k_1 + k_2 G\left(\gamma\right)\right]\phi\right\} + O\left(\phi^2\right) = \alpha\, \eta_0 + O\left(\phi^2\right) \, , \tag{16}$$

with

$$G(\gamma) = \frac{\gamma \mathcal{L}(\gamma)}{4 + 2\,\gamma\mathcal{L}(\gamma)} \tag{17}$$

and

$$\alpha = 1 + \left[k_1 + k_2 G\left(\gamma\right)\right]\phi \, . \tag{18}$$

The constants in Eq. (18) are $k_1 = 5/2$ and $k_2 = 3/2$. If $\gamma \to 0$ implies $G \to 0$, then only the hydrodynamic effect over the viscosity remains.

2.1 Dimensionless equations

Equations (5), (9) and (11) can be made dimensionless defining appropriate scales. A typical scale U is used as velocity scale, the tube radius R as a length scale, R/U as a characteristic time scale and ρU^2 as the pressure scale.

The non-dimensional evolution magnetization equation corresponding to Eq. (9) is:

$$\hat{\omega}\boldsymbol{\Omega} \times \boldsymbol{M} = \boldsymbol{M} - \boldsymbol{M}^o \, , \tag{19}$$

Note that all variables are now dimensionless. In Eq. (19) the parameter $\hat{\omega}$ is the dimensionless magnetization relaxation time defined as

$$\hat{\omega} = \frac{U\,\tau_s}{R} \, . \tag{20}$$

This parameter represents the ratio between the magnetization relaxation time τ_s and the characteristic time of the flow R/U.

The dimensionless forms of Eqs. (10) and (11) are found to be, respectively

$$\nabla \cdot \boldsymbol{u} = 0 \, , \tag{21}$$

and

$$\frac{\partial \boldsymbol{u}}{\partial t} + \boldsymbol{u}\cdot\nabla\boldsymbol{u} = -\nabla p + \frac{\alpha}{Re}\nabla^2\mathbf{u} + C_{pm}\boldsymbol{M}\cdot\nabla\boldsymbol{H} \, , \tag{22}$$

where Re is the Reynolds number based on the ambient fluid viscosity

$$Re = \frac{\rho\, U R}{\eta_0} \, . \tag{23}$$

The parameter α defined in Eq. (18) has been used to correct η^*. The new parameter C_{pm} that appears in the term associated with the magnetic forces is called magnetic pressure coefficient and is defined as (Cunha et al., 2002)

$$C_{pm} = \frac{\mu_0 H_0^2}{\rho U^2} \, . \tag{24}$$

While the Reynolds number measures the relative intensity of the inertial and viscous mechanisms of momentum transport, the magnetic pressure coefficient states for the relative importance of the magnetic pressure compared to the dynamical pressure of the flow, i.e. magnetic effect relative to hydrodynamic effect in the flow field. Note that if $C_{pm} << 1$ the Eq. (22) reduces to the conventional Navier-Stokes equation.

3. Numerical modelling

The governing equations were discretized by using a finite volume scheme. The variables were evaluated in a colocated 2D quadrilateral cartesian structured grid. A regular grid of 100×40 of control volumes (i.e. 10×1 dimensionless units) in 2D was used to solve the velocity, pressure field and magnetic properties for steady applied field conditions. A more refined mesh with 300×60 (i.e. 20×1) control volumes was required for capturing the flow response to a forcing alternating magnetic field.

The magnetic boundary conditions to solve Eq. (5) are Neumann conditions for the prescribed magnetic field. The continuity of the normal component of the magnetic induction vector and the continuity of the tangential component of the field intensity vector on the boundaries of the computational domain are also prescribed. The external magnetic field is considered in a particular region of the pipe.

The fluid velocity on the fixed walls vanishes. A prescribed parabolic velocity profile $u(r) = U(1 - r^2/R^2)$ is used at inlet, where U was set the unit value. In this case a pressure equation is needed to be solved during the numerical procedure. On the other hand when a pressure gradient $\mathcal{G} = -\frac{\partial p}{\partial z}$ is imposed no-inlet condition is needed.

The discretized momentum equation, the magnetic potential equation and the magnetization evolution equation are solved simultaneously. The magnetic force $C_{pm}\boldsymbol{M} \cdot \nabla \boldsymbol{H}$ is treated as a source term in the discretized momentum equations and an explicit treatment scheme is used for modeling the magnetization divergent term in Eq. (5).

The magnetization evolution equation (19) falls into a system of algebraic equations for $\boldsymbol{M}$ components and the fluid vorticity is calculated by using velocity interpolation on the cell faces.

A upwind difference scheme (UDS) is used to predict the convective fluxes at the control volume faces and central difference scheme (CDS) in order to interpolate the diffusive fluxes (Ferziger & Peric, 1997). The velocity at volume control centers is calculated by solving the algebraic system of the discretized form of the momentum governing equation given by:

$$A_P^{u_i} u_{i,P}^m = \sum_K A_K^{u_i} u_K^m + Q_{u_i}^{m-1} - \left(\frac{\delta p^{m-1}}{\delta x_i} \right)_P , \tag{25}$$

where A represents a generic matrix coefficient, m represents the current iteration, $m-1$ denotes the explicit terms, the subscript P denotes the center of an arbitrary control volume, K denotes the neighboring points and Q represents the source terms.

As stated previously the magnetic force is treated in this work explicitly as a source contribution. The source term is simply given in a discretized form by:

$$Q_{u_i} = C_{pm} M_i \frac{\delta H_j}{\delta x_i} . \tag{26}$$

The discretized Poisson equation of the magnetic potential is given by:

$$\frac{\delta}{\delta x_i} \left(\frac{\delta \phi_{mag}^m}{\delta x_i} \right) = -\frac{\delta M_i^{m-1}}{\delta x_i} . \tag{27}$$

The problem of the numerical solution for Eqs.(21) and (22) is the absence of an evolution equation for the pressure. The pressure changes as the velocity evolves in time so the flow field remains non-divergent. Solving the Eq. (25) the continuity equation is not fulfilled, so an equation of pressure correction is needed to ensure mass conservation. The corrected velocity field does not satisfy the momentum equation and an iterative process is performed. The velocity-pressure coupling is solved using the SIMPLE algorithm proposed by Patankar & Spalding (1972). An equation for the pressure correction is obtained by substitution of $u = u^* + u'$ and $p = p^* + p\,'$ into Eq. (22), taking the divergence of Eq. (22) and using the fact that the divergence of the updated velocity field u^m must vanish. The superscription "$*$" and " $'$ " denotes respectively the non-corrected variables and the correction increments.

Time evolutions are made by using an Euler implicit procedure and the unsteady derivative term is treated as a source contribution. This procedure leads to a slightly change in the velocity of the fluid when the time step Δt is sufficiently small compared with the relevant diffusive time R^2/ν (where $\nu = \eta/\rho$) of the flow and with a characteristic period of the magnetic forcing $1/n_f$, where n_f is the forcing frequency of an oscillatory magnetic field. In dimensionless terms this condition is given by:

$$\Delta t < min\left(10^{-2}, Re^{-1}, n_f^{-1} U R^{-1}\right) . \tag{28}$$

The value $\Delta t = 10^{-2}$ in Eq. (28) is the maximum dimensionless time step used in our simulations. More details of the numerical procedure are given in Ramos (2004).

4. Results

The validation of our numerical scheme has been carried out in Ramos et al. (2004, 2005) in which the numerical results were compared with recent asymptotic predictions described in Cunha & Sobral (2004). In particular, the effect of the magnetic pressure coefficient C_{pm} over the magnetic fluid flow was explored in Ramos et al. (2004, 2005). Now we are interested in investigating the influence of the particle volume fraction ϕ and the magnetization relaxation time $\hat{\omega}$ on the magnetic fluid under conditions of steady magnetic field. We also have examined flow bifurcations under oscillating applied fields in order to determine the spectrum of pressure fluctuations and typical amplitudes of velocity-pressure fluctuations.

4.1 Flow under a steady magnetic field

The external magnetic field is given by Eq. (29) in cylindrical coordinates.

$$H_0(z) = \begin{cases} 0 & \text{if } z < z_0 \ ; \\ (z - z_0)\frac{\partial H_0}{\partial z} & \text{if } z \geq z_0 \ . \end{cases} \tag{29}$$

Here z_0 is the position in z coordinate from which the steady magnetic field is applied and the field gradient is constant $\partial H_0/\partial z = 1$. The entire pipe length in our simulations is $L = 20R$.

The presence of particles supplies an increase in the energy necessary to the fluid deformation. In a static magnetic field, the viscosity raises due to the microstructural anisotropy produced by the orientation of the magnetic particles with the field direction that competes with the rotation of the particles induced by the vorticity action.

Whether an axial uniform magnetic field is acting on a pressure driven flow no magnetic force is present. Under this condition the viscosity increasing is a result of the hydrodynamic interaction between the magnetic particles. The effect of the particle volume fraction on the velocity profile is presented in Fig. (1).

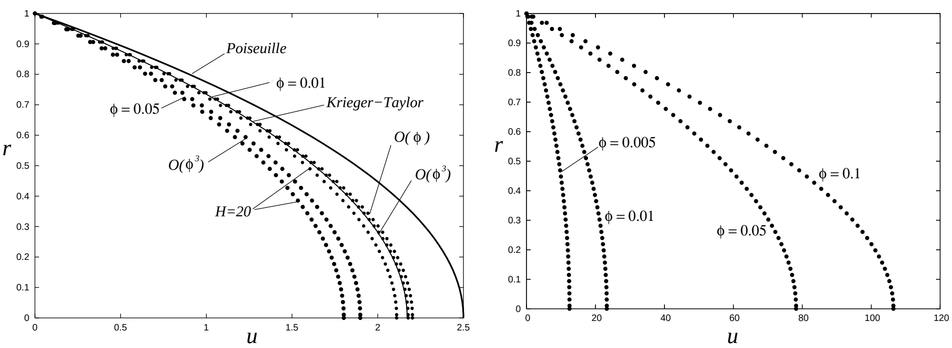

Figure 1. The influence of the magnetic fluid viscosity on the velocity profile for $Re = 10$, $C_{pm} = 10$, $M_d = 100$ and $\mathcal{G} = 1$ for two particle volume fractions $\phi = 0.01$ and $\phi = 0.05$ (a). In figure (a) is shown η^* at $O(\phi)$, $O(\phi^3)$ and the also the empirical Krieger-Taylor equation. The effect of the particle volume fraction ϕ on the velocity profile for a steady non-uniform magnetic field is shown in (b).

The plot in Fig. (1a) shows velocity profile $u = u(r)$ for $Re = 10$, $C_{pm} = 10$, $M_d = 100$, $\mathcal{G} = 1$ for different particle volume fractions. In this figure the binomial expansion for η^* at leading order $O(\phi)$, and at $O(\phi^3)$ and the empirical formula given in Eq. (13) are plotted for a flow condition in which the magnetic field was absent. The influence of an uniform magnetic field is also observed in Fig.(1a). The decrease of the flow rate from the magnetic particle orientation for $\phi = 5\%$ due to an applied magnetic field is approximately 20% compared with the flow in the absent of particles (Poiseuille flow, $\phi = 0$). This difference increases for higher ϕ. The variations in the velocity profile is about 1% between the results based on η^* $O(\phi)$ and $O(\phi^3)$, for $\phi = 0.01$. Viscosity suffers a little increase when the magnetic field is present and the difference between the maximum velocity (i.e. at $r = 0$) considering terms up to $O(\phi^3)$ with no-magnetic field and $H = 20$ (uniform) is approximately 3% for $\phi = 0.05$. Such applied field was imposed in order to guarantee the magnetic saturation of the suspension.

In the presence of a stationary non-uniform magnetic field with $\partial H/\partial z = cte \neq 0$, the magnetic force $C_{pm}\boldsymbol{M} \cdot \nabla \boldsymbol{H}$ becomes non-zero and the equilibrium magnetization $\boldsymbol{M}^o$ increases with the particle volume fraction. Figure (1b) shows the ϕ influence on the velocity distribution in a flow with non-zero magnetic force. It is seen that a positive magnetic force increases the mean velocity even for an increasing in the viscosity of the magnetic fluid. From a practical point of view, this result suggests the possibility of using oriented magnetic particles in a carrier fluid for reducing drag even in laminar flow.

The dimensionless magnetization relaxation time $\hat{\omega}$ is a very small parameter in ferrofluids. However in magnetic rheological suspensions the micro-size particle might be greater than typical particles of nano-suspensions, being possible have $\hat{\omega} \sim 0.1$ in dilute solutions of super-paramagnetic micro-particles. Figure (2) shows the influence of $\hat{\omega}$ on the flow for several values of the dimensionless relaxation times. In a magnetic fluid with $\hat{\omega} > 0$, the vorticity $\boldsymbol{\Omega}$ influence becomes stronger such as stated in Eq. (19). Since $\boldsymbol{\Omega}$ and $\boldsymbol{H}$ are not parallel, the balance between vorticity and particle polarization attenuates the magnetization contribution on the resulting magnetic force.

4.2 Drag reduction

Whether no-pressure gradient is specified down the tube the pressure-velocity coupled needs to be solved. In the absence of magnetic fields pressure decays linearly ($\mathcal{G} = -\frac{\partial p}{\partial z} \geq 0$) for a prescribed mass flux (Poiseuille flow). When $\nabla \boldsymbol{H}$ is in the same direction of $\mathcal{G}$ the pressure field adjusts to the new condition in order to maintain the flow rate. A drag reduction can be quantify by defining f_r as the friction factor reduction, namely

$$f_r = \frac{f^H - f^0}{f^0} \ , \tag{30}$$

where f^H is the friction factor calculated in the domain in which the magnetic field is present and f^0 if the friction factor corresponding to the no-magnetic field region. Figure (3) presents f_r as function of the magnetic pressure coefficient for $\phi = 0.01$, $Re = 10$, $\hat{\omega} = 0.01$

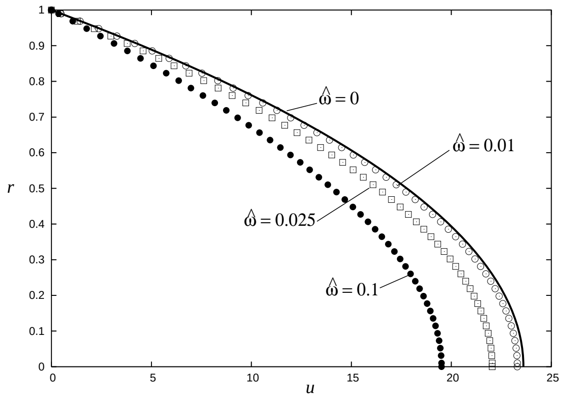

Figure 2. Dimensionless magnetization relaxation time $\hat{\omega}$ influence on the velocity profile for $Re = 10$, $C_{pm} = 10$, $\phi = 0.01$, $\mathcal{G} = 1$ e $\partial H/\partial z = 1$.

and $M_d = 100$ in a flow with a prescribed volumetric rate at pipe inlet $\dot{Q} = 1$. This result indicates that is possible to reduce the drag in laminar pipe flows using low concentrations of magnetic particles in the presence of applied magnetic fields. This possibility is a direct consequence of the anisotropy produced by the orientated particles that exerts an extra force on the flow. The action of this force in the favorable direction of the flow is reflected as being an increasing in the volumetric rate. The variation of $|f_r|$ as a function of C_{pm} shown in the plot of figure (3) is well fitted by the following power law $|f_r| = C_{pm}^{19/20}$.

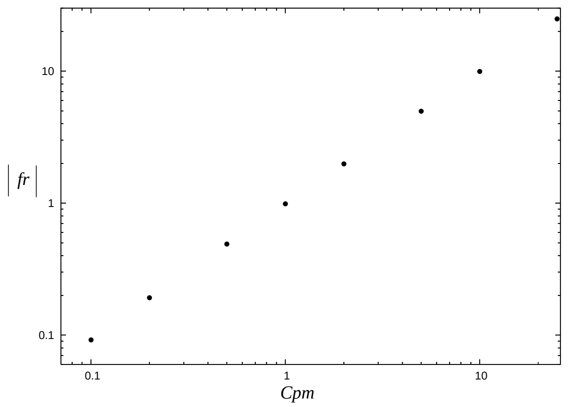

Figure 3. Friction factor reduction $|f_r|$ as a function of the magnetic pressure coefficient C_{pm} for $\dot{Q} = 1$, $Re = 10$, $\phi = 0.01$, $\hat{\omega} = 0.01$ and $M_d = 100$.

4.3 Nonlinear-frequency response

We are now interested in examining the flow response under condition of an imposed unsteady magnetic boundary condition. The oscillatory magnetic field is given by

$$H_0(z,t) = \begin{cases} 0 & \text{for } z < z_0 \ ; \\ (z - z_0)\frac{\partial H_0}{\partial z} \ \cos\omega t & \text{for } z \geq z_0. \end{cases} \quad (31)$$

where $\partial H_0/\partial z = 1$, $\omega = 2\pi/\mathcal{T}$ and $\mathcal{T}$ is the oscillation period of the harmonic applied field. Note that for $\omega = 0$, the external magnetic field reduces to an imposed stationary field. The time-average field for a period of oscillation in Eq. (31) is zero and in this case the magnetic force is always positive.

In addition, a second condition in which the time-average field is not null and the resulting magnetic force is alternating is also simulated:

$$H_0(z,t) = \begin{cases} 0 & \text{for } z < z_0 \ ; \\ \left[(z - z_0) - \frac{L_H}{2}\right] \frac{\partial H_0}{\partial z} \cos\omega t + \frac{L_H}{2} & \text{for } z \geq z_0, \end{cases} \quad (32)$$

where L_H is the pipe length under the external applied field. Some results of the frequency response of the flow under oscillatory magnetic fields have been shown recently in Ramos et al. (2004, 2005).

In a pipe flow with a constant volumetric rate where external boundary conditions are unsteady the pressure distribution changes with time. Figure (4) shows the time-series and phase-diagrams for a magnetic fluid flow undergoing an external magnetic field specified in Eq. (32) with a dimensionless frequency $n_f = 100$ (where $n_f = 1/\mathcal{T}$) for different C_{pm}. It is seen that at higher frequencies the

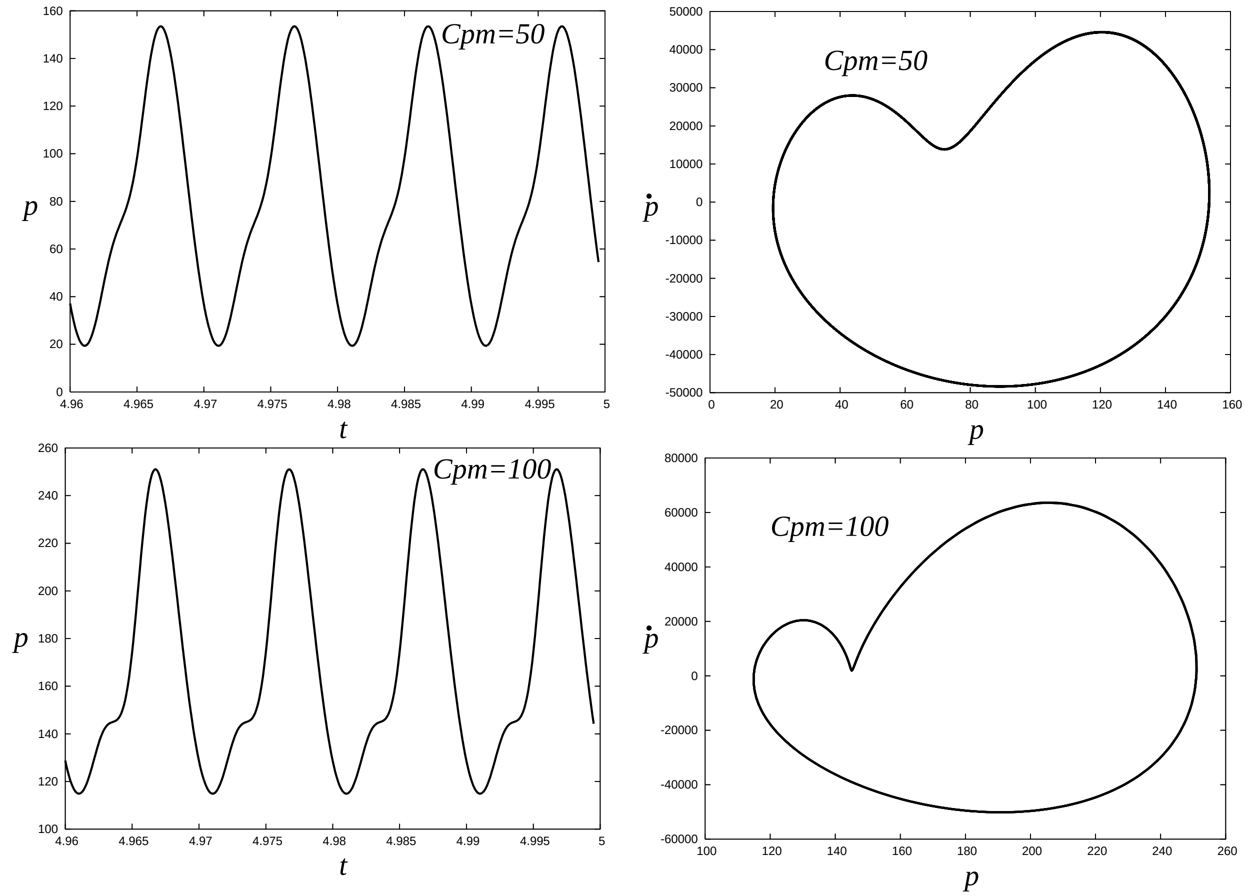

Figure 4. Time-series and pressure phase-diagrams for $C_{pm} = 50$ and $C_{pm} = 100$ with $z = 18$, $r = 0$ e $n_f = 100$, $Re = 10$, $Md = 100$, $\phi = 0.01$ and $\hat{\omega} = 0.01$.

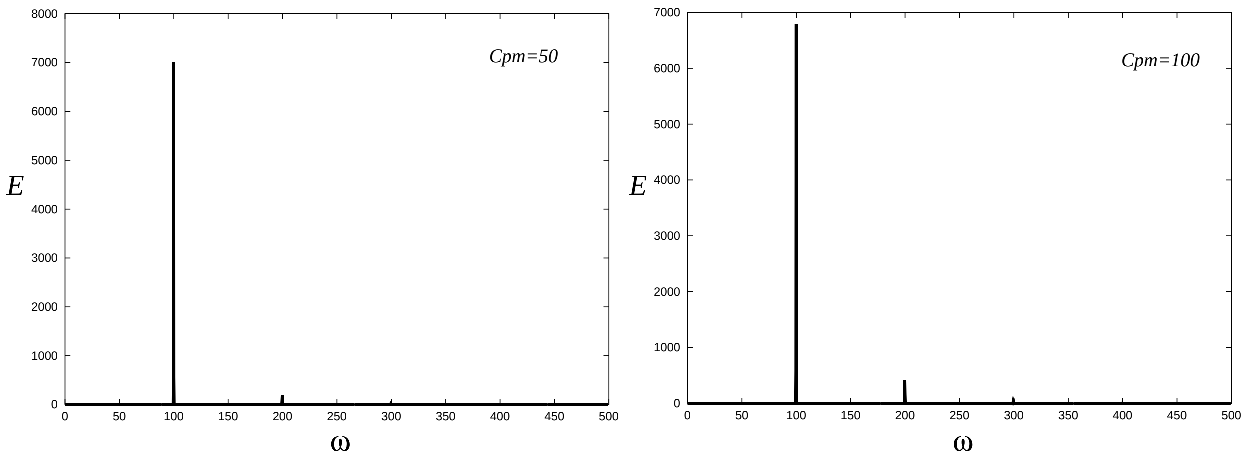

Figure 5. Power spectrum of the pressure fluctuations for $C_{pm} = 50$ and $C_{pm} = 100$ with $n_f = 100$, $Re = 10$, $C_{pm} = 50$, $z = 18$, $r = 0$, $Md = 100$, $\phi = 0.01$ and $\hat{\omega} = 0.01$.

flow response may drastically deviate from the simple harmonic behavior of the applied magnetic field. The flow becomes nonlinear and bifurcations arises as a consequence between the strong coupling of the flow with the particle magnetization.

Figure (5) depicts the power spectrum of the pressure fluctuation for $C_{pm} = 50$ and $C_{pm} = 100$ under the same physical conditions of Fig. (4). The plot presents the fluctuation intensities E as function of the oscillating modes. Two significant oscillating modes can be identified from the power spectrum of the pressure fluctuations. The principal mode corresponds to the the same frequency of the imposed oscillatory field ($n_f = 100$). The extra nonlinear modes occurs at the frequency $2n_f$. A third small mode associated to the frequency $3n_f$ arisen when $C_{pm} = 100$. We see that the intensity of the second harmonic increases more than 100% when comparing the value of E for $C_{pm} = 50$ with its corresponding value for $C_{pm} = 10$ at same forcing frequency, n_f. This indicates that for higher C_{pm} the coupling between the flow and the magnetic field may becomes strongly nonlinear, resulting flow bifurcations and unstable flow configurations.

4.4 Velocity fluctuations

The velocity field behavior under an imposed oscillatory magnetic field defined in Eq. (31) is better observed in a pressure driven pipe flow with constant $\mathcal{G} = 1$. Now, the time-average velocity $\overline{u(r)}$ is defined as

$$\overline{u(r)} = \lim_{t\to\infty} \frac{1}{t} \int_{t_0}^{\infty} u(r,t)\,\mathrm{d}t\,. \tag{33}$$

where t_0 denotes a dimensionless time which is taken sufficiently long in order to hold the full decaying of the transient part of the flow response. The associated velocity fluctuations are calculated by the expression

$$\left(\overline{u(r)'^{\,2}}\right)^{\frac{1}{2}} = \lim_{t\to\infty} \left\{ \frac{1}{t} \int_{t_0}^{\infty} \left[u(r,t) - \overline{u(r)}\,\right]^2 \mathrm{d}t \right\}^{\frac{1}{2}}, \tag{34}$$

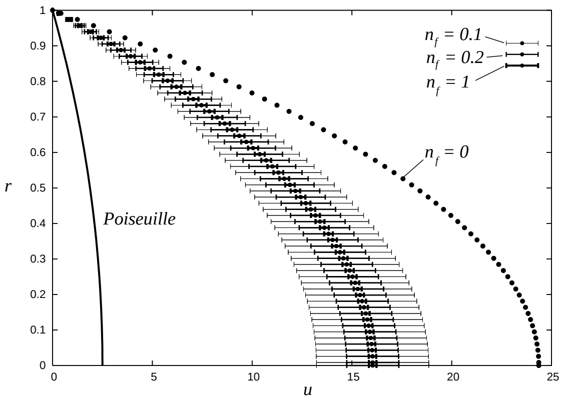

Figure 6. Time-average velocity profile. $Re = 10$, $C_{pm} = 10$, $\mathcal{G} = 1$. The prescribed magnetic field is defined in Eq. (31).

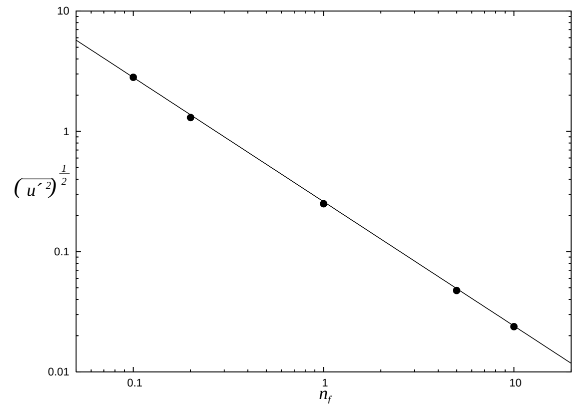

Figure 7. Velocity fluctuation amplitude versus oscillation frequency n_f with $r = 0$. $Re = 10$, $C_{pm} = 10$, $\mathcal{G} = 1$. Solid line represents the power law fit $(\overline{u'^{\,2}})^{\frac{1}{2}} = \frac{1}{4}\, n_f^{-103/100}$. The prescribed magnetic field is defined in Eq. (31).

Figure (6) presents the time-average velocity profiles for $Re = 10$ and $C_{pm} = 10$ for several n_f values. The maximum velocity decreases approximately 30% for $n_f \sim 10$ in relation to the corresponding values for $n_f = 0$ condition. In general, we find velocity fluctuations decaying as increasing n_f. It is seen that hight variation rates of the imposed field are not followed by the velocity response. The period of the forcing magnetic field $(1/n_f)$ is indeed much smaller than a typical time scale of the flow, say $\tau_f = (R/(\overline{u'^{\,2}})^{-\frac{1}{2}})$. Therefore at very hight values of n_f the flow does not have a sufficient time to respond to the imposed field oscillations and consequently the velocity fluctuations are indistinguishable from zero. In this case the unsteady hydrodynamic-magnetic coupling is just a weak effect on the flow. In addition, as the simpler measure of a flow instability is the velocity fluctuation intensity, we argue that under high frequency of an imposed field the flow response would be stable for a specified pressure gradient. Here, for a forcing frequency $n_f = 100$ a typical time scale of the velocity fluctuations $\tau_f \sim 1000$, that is much long then the forcing time scale 0.01. Finally, the plot in fig. (6) suggests a power-law fit of the velocity fluctuations as a function of the forcing frequency given by $(\overline{u'^{\,2}})^{\frac{1}{2}} = \frac{1}{4}\, n_f^{-103/100}$.

5. Final remarks

In this article we have reported numerical simulation results for the flow of a magnetic fluid in a cylindrical tube. The simulations all were based on a finite volume scheme that has been developed for computing the motion of such complex fluid in two-dimensional and axisymmetric flows. We have seen that the particle volume fraction can enhance the volume rate even with the effective viscosity of the fluid increasing due to the presence of the oriented magnetic particle. We have found this possible whether the imposed magnetic gradient is applied in the same direction of the favorable pressure gradient. A positive magnetic force proportional to the field gradient can promote a drag reduction in the flow such as shown in the result of the friction factor as a function of the magnetic pressure coefficient. The numerical scheme was able to capture nonlinear frequency response in the flow of a magnetic fluid under condition of alternating magnetic fields. High frequencies tend to make the pressure response nonlinear with appreciable pressure fluctuations and at least three modes of oscillations identified at frequencies n_f, $2n_f$ and $3n_f$. On the other hand the small observed velocity fluctuations were a result of the weakly coupling between the velocity response and the imposed oscillatory field produced by a large difference (i.e. al least five order of magnitudes) between the time scales of the forcing and the velocity fluctuation response.

6. Acknowledgements

We are thankful to FINATEC-DF, CAPES and CNPq for the financial support given to this project.

7. References

Barnes, H. A., Hutton, J. F., K. Walters, F. R. S., 1989. "An Introduction to Rheology", Elsevier Science Publichers Comp. Inc., New York.

Berthier, J., Ricoul, F., 2002. "Numerical Simulation of Ferrofluid Flow Instabilities in a Capillary Tube at Vicinity of a Magnet", Modeling and Simulation of Microsystems, http://www.cr.org, ISBN 0-9708275-7-1.

Cunha, F. R., Sobral, Y. D., 2004. "Characterization of the Physical Parameters in a Process of Magnetic Separation and Pressure Driven Flow of Magnetic Fluid", Physica A, Vol. 343, pp. 36-64.

Cunha, F. R., Sousa, A. J., Morais, P.C. 2002. "The dynamic behavior of a collapsing bubble in a magnetic field", J. Magn. Magn. Mater, Vol. 252, pp. 271. 36-64.

Einstein, A., 1956. "Investigations on the theory of the Brownian Movement", Dover Publications, New York.

Fannin, P. C., 1994. "An Experimental Observation of the Dynamic Behavior of Ferro-fluids", Journal of Magnetism and Magnetic Materials, Vol. 136, pp. 49-58.

Felderhof, B. U., 2001. "Flow of a ferrofluid down a tube in an oscillating magnetic field", Phisical Review E, Vol. 64.

Ferziger, J. H., Peric, M., 1997. "Computational Methods for Fluid Dynamics", Springer-Verlag, Berlim.

Kamiyama, S., Koike, K., 1992. "Hydrodynamics of Magnetic Fluids", Tohoku University, Japan.

Oldenburg, C. M., Borglin, S. E., Moridis, G. J., 2000. "Numerical Simulations of Ferrofluids for Subsurface Environmental Engineering Applications", Transport in Porous Media, Vol. 38, pp. 319-344.

Patankar, S. V., Spalding, D. B., 1972. "A Calculation Procedure for Heat, Mass and Momentum Transfer in Three-dimensional Parabolic Flows", Int. J. Heat Mass Transfer, Vol. 15, p. 1787.

Ramos, D. M., 2004, "Modelagem e Simulação Numérica da Hidrodinâmica de Fluidos Magnéticos em Movimento", Dept. Mech. Eng / FT, Unversity of Brasília, Dissertation, DM-71.

Ramos, D. M., Sobral, Y. D., Cunha, F. R., Rodrigues, J. L. A., 2004. "Numerical simulation of magnetic fluid flows by a Finite Volume Method", Proceedings of the 10th Brazilian Congress of Thermal Sciences and Engineering – ENCIT 2004

Ramos, D. M., Sobral, Y. D., Cunha, F. R., Rodrigues, J. L. A., 2005. "Computer simulations of magnetic fluids in laminar pipe flows", Journal of Magnetism and Magnetic Materials, Vol. 289, p. 238.

Rosensweig, R. E., 1997. "Ferrohydrodynamics", Dover Publications Inc., New York.

Schumacher, K. R., Sellien, I., 2003. "Expeiment and Simulation of Laminar and Turbulent Ferrofluid Pipe Flow in an Oscillating Magnetic Field", Physical Review E, Vol. 67.

Shiliomis, M. I., Morozov, K. I., 1994. "Negative Viscosity of Ferrofluid under Alternating Magnetic Fluid", Phys. Fluids, Vol. 6, pp. 2855-2861.